

Biocompatibility of SLS-Formed Calcium Phosphate Implants

G. Lee*, J.W. Barlow*, W.C. Fox**, and T.B. Aufdermorte***

*Department of Chemical Engineering
The University of Texas at Austin
Austin, Texas 78712

**BioMedical Enterprises, Inc.
14785 Omicron Dr., Suite 205
San Antonio, Texas 78345-3201

***Department of Pathology
The University of Texas Health Science Center at San Antonio
San Antonio, Texas 78284

Abstract

A method for fabricating artificial calcium phosphate bone implants by the Selective Laser Sintering (SLS) process has been developed that can fabricate complex and delicate calcium phosphate bone facsimiles from a variety of data inputs including Computed Tomography(CT) files (1). This paper discusses two *in vivo* biocompatibility studies of SLS-formed calcium phosphate implants in both rabbits and dogs. Histologic analysis shows a high degree of biocompatibility and bone ingrowth in both studies.

Introduction

Much attention has been given to develop materials that can assist in the regeneration of bone defects and injuries (2). Although efforts has been great in developing a biocompatible material, little research has been done toward the rapid and automated shaping of replacement bones using these materials. A human body is composed of 206 different bones and every bone is different in size from person to person. Specially, bones in craniofacial or maxillofacial area are prone to be very complex in shape as well as vary in size. For example, reconstruction of the oral cavity could benefit from an implant that matched the shape of the patient's original anatomy, fit the defect and guided the regeneration of the soft tissue.

As described earlier, we developed a process that uses SLS to form complex geometries from calcium phosphate powders (1). This process, coupled with the well established medical imaging technology of Magnetic Resonance Imaging (MRI) and CT, can precisely reproduce accurate facsimiles of any skeletal bone. The present study examines the biocompatibility of implants made by this process in rabbit and dog animal models.

Materials and Methods

Powder preparation Monocalcium phosphate, monohydrate (MCP, Food grade) and Dicalcium Phosphate Anhydrous (DCP/A, USP/FCC grade) were obtained from Rhone-Poulenc Basic Chemical Co. as raw materials. Specimens with Ca/P ratio of 0.5 to 0.9 were formed in a two step process. The first step involved the mechanical mixing of MCP and DCP/A in such a way that the resulting powder contained a Ca/P ratio of 0.9. For example, 0.8 mole of DCP/A and 0.2 mole of MCP were mechanically mixed and fired at a controlled temperature about 950 °C to obtain a solid solution of β -calcium pyrophosphate (3), β -2CaO•P₂O₅. The resultant sintered cake was then either ball milled or ground by mechanical blender, and selectively sieved to obtain powders with particle size less than 75 μ m.

Following previously established procedures (4), a poly(methylmethacrylate-co-n-butyl methacrylate) latex polymer was synthesized as a binder. The melt flow index of polymer was tailored about 7.7 g/10 min. at 200 °C and 75 psi, as measured by a Kayness Galaxy I capillary rheometer. This flow range had been previously discovered to allow the binder to flow and rapidly wet the inorganic material under SLS process conditions.

Calcium phosphate powder was coated with polymer by spray drying a slurry of particulate and emulsion binder. The spray drier used in this study is a pilot -plant scale Anhydro Laboratory Spray Drier # 1 with co-current rotary atomizer. This spray drying process produces a free flowing powder that has the desired agglomerated morphology. Spray drying condition were as follows. Solids content of slurry was 45 wt. %, inlet temperature, 175°C, outlet temperature, 110°C, and atomizer speed was above 30,000 rpm. Polymer content in coated powder was 22 wt. % as determined by Thermal Gravimetric Analysis (TGA).

SLS processing Spray dried material were processed using a beta test workstation SLS™ Model 125 equipped with modulated 25 W CO₂ laser. Laser output power, beam scan speed, scan spacing and powder bed temperature were controlled to optimize the green strength according to the shape of the implants. Optimal settings for *Energy Density* (5) were found to be in the range of 1 to 1.5 cal/cm².

Post Processing SLS-formed green objects were infiltrated with calcium phosphate solution, fired to remove the polymeric binder, then fired at higher temperature to sinter the calcium phosphate particles. The parts were subsequently infiltrated with DCP/A solutions in diluted phosphoric acid by submersing them in the solutions. The capillary action of the pores drew the infiltration solution into the part. After the pores were filled with infiltrant, the parts were allowed to dry prior to firing. The firing temperatures were controlled to be lower than the initial sintering temperature to avoid further shrinkage, but high enough to provide atomic diffusion and chemical reactions to occur between Ca and P in the infiltrant and that of the green part. When the green part was first infiltrated, the Ca/P ratio and solids content of the infiltrant were chosen to facilitate a clean burn out of polymer. After debinding, the extent of infiltration and the concentration of the infiltrant

were varied to achieve desired density, pore structure, mechanical strength and a final Ca/P ratio. This approach allowed the density of the final product and its chemistry to be precisely controlled in the final firing step.

Material characterization The effect of post processing on calcium phosphate chemistry was studied by X-ray diffraction. The microstructure of the prepared specimen was evaluated by mercury porosimetry and scanning electron microscopy (SEM). The SEM was primarily used to visualize surface morphology and the internal structure of samples.

The pore structure of the *in vivo* oral implant, described below, was measured by mercury porosimetry (Poresizer 9320, Micromeritics). Prior to porosimetry measurements, the oral implant was heated to expel the absorbed moisture and then stored in a desiccator until analyzed. The sample in the Poresizer was initially evacuated to 25 $\mu\text{m Hg}$. Mercury was then admitted and pressure was increased up to 30,000 psi. Assuming a contact angle of 130 $^\circ$ (6), pore diameters ranging from 200 to 0.006 μm were measured. Figure 1 shows a typical pore size distribution. From mercury intrusion analysis, the total pore area 1.82 m^2/g and median pore diameter 33 μm were measured. The measured porosity was about 30 %, which is smaller than the observed value, about 50 %, from geometrically-based density measurements. This could indicate that some closed pores are present in the part.

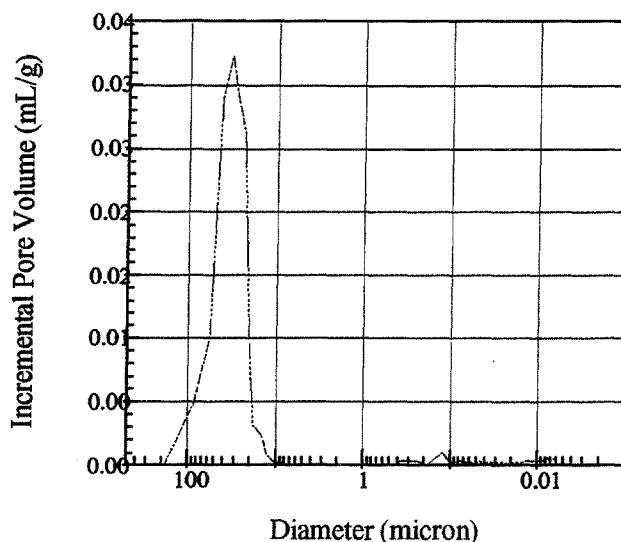


Figure 1. Pore size distribution of oral implant

Two test methods, compression and 4-point bending, were used to quantify the strength of the specimens by a MTS Sintech 1/S material test frame. Typical strengths are in the range 2,000 psi in compression and 2,200 psi in 4-point bending.

Implant preparation and animal studies. Preliminary *in vivo* biocompatibility studies were carried out with rabbits. Tiny rectangles, 0.12" x 0.16" x 0.05", were prepared by a process that simulated SLS process conditions. Calcium metaphosphate was mixed with

the same polymeric binder used previously (1) and poured into the cavity of the mold without compaction. The mold was heated to form polymer-bound "green" parts. The green parts were then fired at about 920°C to remove the binder and to sinter the calcium phosphate. One of the prepared calcium phosphate specimens was implanted over the frontal lobe of the skull in each of four New Zealand White Rabbits. The cortex of each skull was decorticated to cause minor hemorrhage and create a small defect in which the implant could rest. At twelve weeks the animals were sacrificed. Implants and bone were retrieved and embedded in plastic, sectioned and analyzed.

More elaborate *in vivo* biocompatibility studies were carried out in dogs. Anatomical measurements of the original geometry of the dog alveolar ridges were taken to determine their anatomy. AutoCad engineering computer-aided design software was then used to design the oral implants. These implants were rectangular shaped and tapered so as to decrease their buccal-lingual width apically, see Figure 2. The sides and bottom of these implants had large hexagonal macropores of about 2.4mm that penetrated entirely through the device. These macropores were aligned so they intersected within the implants. Tooth extraction of the first mandibular molar bilaterally was performed in six dogs and bone was cut from the extraction site to prepare a defect in the alveolar ridge. The first molar was extracted bilaterally from the mandible. Primary closure was achieved and the dogs were allowed to heal for eight days. After the 8-day healing period, the extraction defect in the alveolar ridge was surgically exposed. Implants were placed in the ridge and primary closure was achieved. Dogs were put on soft food for the duration of the study. Radiography was performed to obtain data giving an indication of the implants osteoconductive properties and its biocompatibility. Radiographs were taken immediately post-operatively and at four weeks into the study.

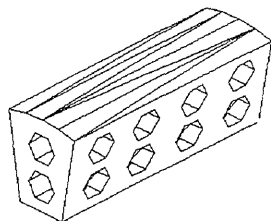


Figure 2. Designed oral implant

Results and Discussion

A histologic section of the calcium phosphate implant after twelve weeks implantation in rabbit's frontal skull is shown in Figure 3. The implant shows a high degree of biocompatibility and bone ingrowth. No evidence of foreign body giant cell or macrophage response was found in or adjacent to the specimen. There was no acute or chronic inflammation, and a high degree of bone apposition and infiltration is observed. Mineralized new bone is present throughout a significant portion of the implant closest to the underlying calvaria. Osteoid, or a collagen matrix with bone forming potential, fills the majority of the rest of the implant. It is suggested from this histology that, in time,

the specimen could be completely filled with dense mineralized bone. A higher magnification of the histologic section is shown in Figure 4. Direct bone apposition and ingrowth are visible across the interface and throughout the implant. Host bone is directly connected to bone within the implant providing good mechanical stability.



Figure 3. Histologic section of implants taken overlying the rabbit calvaria. (40x original magnification)

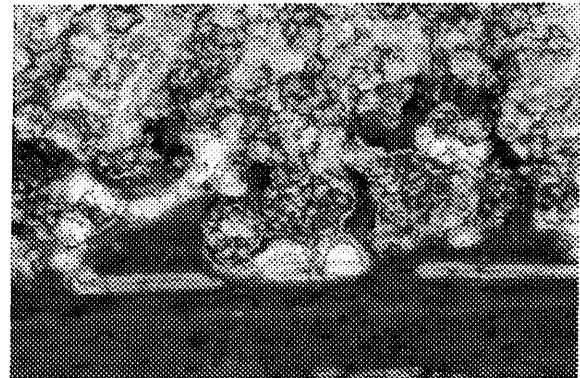


Figure 4. Histologic section of implant taken overlying the rabbit calvaria (100x original magnification)

A scanning electron micrograph of surface of the SLS formed oral implant is shown in Figure 5. This surface is imaged at 150 times of the original magnification and 100 μm measure is visible in the lower right of the image. In Figure 6, the polished surface is shown at the same magnification. It is clear from these pictures and mercury intrusion analysis, that some of the pores are larger than 100 μm and that the pores are open and well interconnected. These issues are critically important to the successful development of a osteoconductive bone implant material. It is known that mineralized bone growth into porous implants required a minimum interconnected pore size of 100 μm , and the pore size showing the potential for the ingrowth of osteoid tissue, was found to lie between 40 and 100 μm (7).

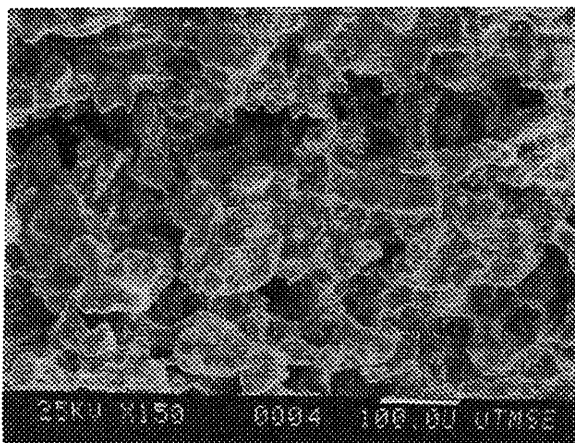


Figure 5. Scanning electron micrograph of the surface of SLS-formed implant.

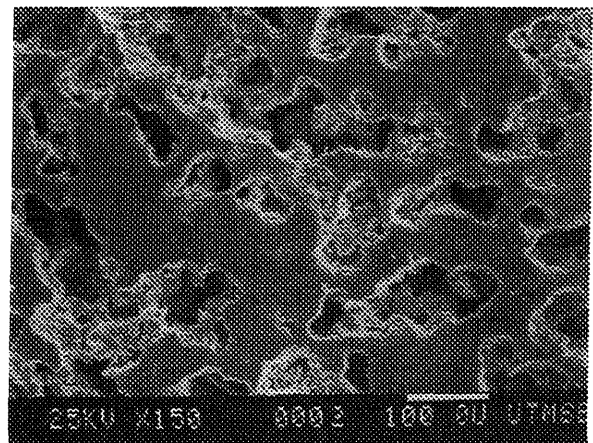


Figure 6. Scanning electron micrograph of a polished surface of SLS-formed implant.

Figure 7 shows the periapical radiograph of a SLS-formed alveolar implant. This image was taken immediately post-operative. The rectangular form of the implant and hexagonal form of the macropores are visible in this radiograph. In Figure 8, a radiograph image taken four weeks following placement of the implant is shown. Crestal resorption and bone infiltration into the apical macropores and apical portion of the crestal macropore are evident from the film.

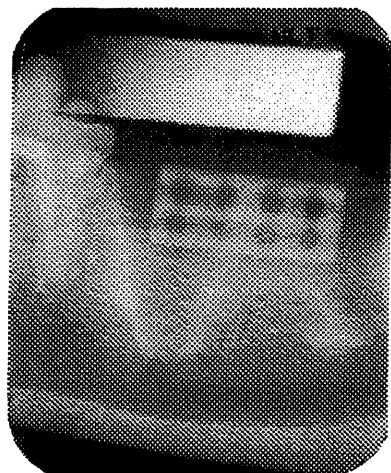


Figure 7. A radiograph of a SLS-formed alveolar implant with micro- and macropores.

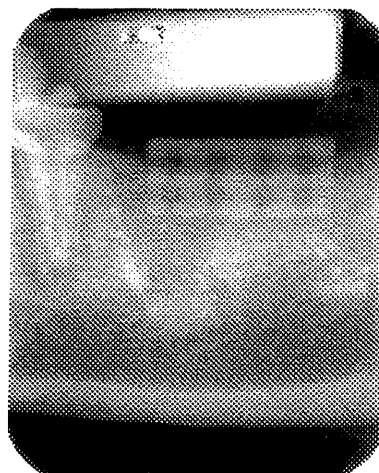


Figure 8. A radiograph of a SLS-formed alveolar implant with micro- and macropores.

As a demonstration of this bone fabrication technique, a human anatomical facsimile was formed from CT images using SLS. This inferior view of the maxilla shows some dentition and anterior nerve and vascular foremen with great resolution.

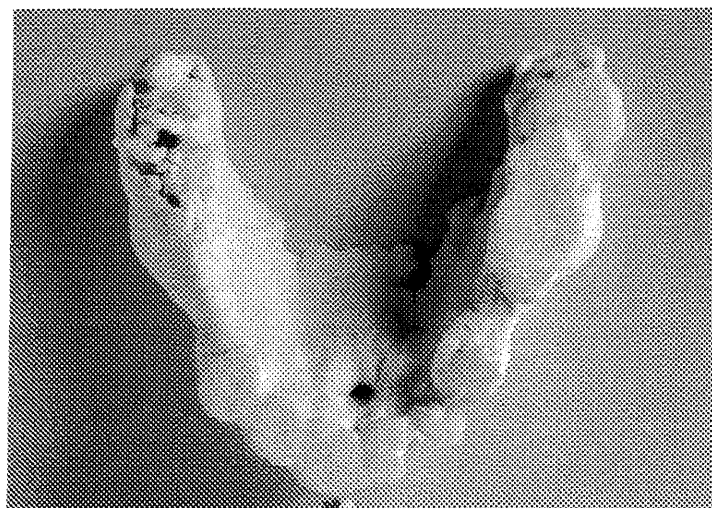


Figure 9: Ca/P human maxilla formed from CAT images using SLS.

Conclusion

Based on the excellent biocompatibility of material and the great extent of bony tissue ingrowth shown in the rabbit *in vivo* study, the calcium phosphate powder system for the SLS process has been established. As a starting material Ca/P ratio 0.9 was synthesized and formed by SLS. Oral implants in alveolar ridges of dogs show excellent integration with host bone after only four weeks of implantation. This study shows that a porous, resorbable calcium phosphate synthetic bone material can be precisely fabricated with complex geometry and successfully used *in vivo* for filling and replacing defective bone.

Acknowledgments

The authors gratefully acknowledge partial support for this work by the State of Texas Advanced Technology Program, No. 265, BioMedical Enterprises, Inc., and the United States Air Force Armstrong Laboratory through contract F41624-95-C-2008.

References

1. G. Lee and J.W. Barlow, "Selective Laser Sintering of Calcium Phosphate Powders," *Solid Freeform Fabrication Symposium Proceedings*, **1993**, The University of Texas at Austin, Texas, pp.191-197.
2. S.F. Hulbert, L.L. Hench, D.Forbes, and L.S. Bowman, "History of Bioceramics," *Ceramics in Surgery* edited by P. Vincenzini, **1982**, Elsevier, Amsterdam, pp 3-29.
3. W.L.Hill, G.T.Faust and D.S. Reynolds, "The Binary System $P_2O_5-2CaO \cdot P_2O_5$," *Am. Jour. Sci.*, **1944**, *242* (9), 457-477.
4. N.K.Vail, *et al.*, "Development of a Poly(methyl methacrylate-co-n-butyl methacrylate) Copolmer Binder System", *J. Appl. Polym. Sci.*, **1994**, *52*, 789-812.
5. J. C. Nelson, *et al.*, "Selective Laser Sintering of Polymer-Coated Silicon Carbide Powders," *Ind. Eng. Chem. Res.*, **1995**, *34*, 1641-1651.
6. E.W. Washburn, "Note on a Method of Determining the Distribution of Pore Sizes in a Porous Material," *Proc. Natl. Acad. Sci.*, **1921**, *7*, pp115-116.
7. J.J. Klawitter and S.F. Hulbert, " Application of Porous Ceramics for the Attachment of Load Bearing Internal Orthopedic Applications," *J. Biomed. Mater. Res. Symposium*, No.2, **1970**, pp161-229.

